On the transport mechanism of energy-coupling factor transporters

Swier, Lolkje Janine Yvonne Marijke

Chapter 6

Reconstitution of ECF transporters in phospholipid bilayer nanodiscs

Lotteke J. Y. M. Swier and Dirk J. Slotboom

Studying membrane proteins purified from their native membrane can be quite problematic, since detergents or model membrane systems do not always provide the required characteristics for the stability and functionality of these proteins. In this chapter, we describe the optimization of reconstitution in a non-compartmentalized model membrane system, the phospholipid nanodisc, for two ECF transporters from different organisms; the ECF NiaX transporter for niacin from *L.lactis* and ECF FolT2 from *L. delbrueckii*. With these transporters reconstituted in nanodiscs, the ATPase activity was studied in the presence and absence of their substrates. The ATPase activity turned out to be four orders of magnitude higher than the transport activity measured in proteoliposomes, and independent of the presence of the substrate. This suggests that cells can afford to hydrolyze extra ATP to make sure that the ECF module is available for interaction with a S-component as soon as it has captured a substrate molecule.

Introduction

The part of a membrane protein that is inserted in the membrane, has a hydrophobic surface and interacts with the hydrophobic tails of the lipids forming the lipid bilayer. When working with purified membrane proteins *in vitro*, they need to be extracted from their native membrane. Hereby, care must be taken to shield the hydrophobic surface from the aqueous solution in which the proteins are put, otherwise they will aggregate. A classical method is to solubilize the membrane protein in detergent, which will form a belt of detergent molecules around the hydrophobic part of the protein and makes it soluble in an aqueous solution. Many different kinds of detergents are available, having ionic (charged), non-ionic (non-charged) or zwitterionic (having both positively and negatively charged groups, with a net charge of zero) head groups and tails with a length ranging from one to sixteen carbon atoms, which can be branched or not, saturated or unsaturated and can contain functional groups.[1] However, detergents are a non-natural environment and often give stability issues. Finding the right detergent that keeps your membrane protein stable, can be tedious, and even then, your protein might not be functional because of the absence of a native-like lipid bilayer. There is the possibility to solubilize your membrane protein in mixed lipid-detergents micelles, but this does not always do the trick.

To solve the stability and functionality issue, membrane proteins are commonly reconstituted in liposomes for functional studies. The resulting proteoliposomes have the membrane protein inserted in a lipid bilayer, of which the composition is controllable, and the size of the proteoliposomes can be more or less controlled by extrusion through polycarbonate membranes with a certain pore size. Besides, the enclosure of the lumen makes it possible to build gradients and to study transport activity. However, upon reconstitution, a mixture of proteins reconstituted right-side out and inside-out is obtained, and none of the proteins is accessible from both sides. Proteoliposomes also have the disadvantage that they are rather big (diameters in the high nanometer to micrometer range), which makes them unsuitable for some types of experiments. Besides, they are sensitive to osmotic changes and compounds that make them leaky, and it is difficult to prepare them with a precise controlled size and protein-to-lipid stoichiometry. In the last thirty years, three new model membrane systems have been developed, being bicelles,[2,3] phospholipid bilayer nanodiscs[4,5] and native nanodiscs.[6] In this chapter, we will focus on the use of the phospholipid bilayer nanodiscs.

The phospholipid bilayer nanodisc consists of a small disc of phospholipid bilayer, which is encircled by two amphipathic membrane scaffold proteins (MSPs) in a head-to-tail belt-like conformation (Figure 1).[4,5,7] These MSPs are modelled after the human serum apolipoprotein A-1, which bundles phospholipids and cholesterol molecules together in disc-like high density lipoproteins (HDLs) that play a role in cholesterol transport.[8,9] Reconstitution of membrane proteins in nanodiscs has many advantages. There has been a range of membrane scaffold proteins engineered, making it possible to form nanodiscs with diameters ranging from 95 to 170 Å.[10–13] The thickness of the bilayer depends on the lipid composition, which is easy to control. Upon reconstitution, the membrane proteins experience a native-like environment which provides stability and functionality requirements, while they are soluble in aqueous solution at the same time.[14,15] The size-restriction by the MSP provides control of the oligomeric state of the protein and ensures to a close-to-homogenous sample preparation, which is reproducible over different batches. The small size of the nanodiscs makes them suitable for many

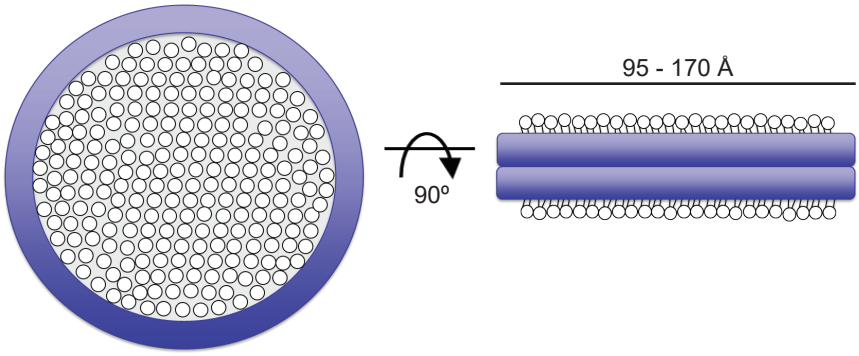

Figure 1: Reconstitution in phospholipid bilayer nanodiscs. Top view (left) and side view (right) of a schematic, not scaled representation of a nanodisc, with the membrane scaffold proteins shown as two dark blue bands that encircle the patch of phospholipid bilayer, of which the phospholipid head groups are represented by white balls and the phospholipid tails by black lines. The bar above the side view indicates the range of diameters that can be obtained using different MSPs.

techniques only applicable to small, soluble particles, and since only one membrane protein is reconstituted per nanodisc under the appropriate condition, this model membrane system is even suitable for single-molecules studies. By modifying the MSPs, the nanodiscs can be immobilized on surfaces as well.

When reconstituting your membrane protein of interest in nanodiscs, time needs to be invested in finding the optimal membrane protein to MSP to lipid ratio for the preparation of the nanodiscs. Based on the diameter of the lipidic discs calculated for the different MSPs, an estimate for the number of lipids needed can be made. However, it is unknown how many of these lipids are replaced upon reconstitution of the membrane protein into the nanodisc. Using high MSP to protein ratios will increase the change of incorporating only one membrane protein per nanodiscs, but lower ratios will decrease the number of empty nanodiscs.[10] If the lipid to MSP ratio is taken too low, lipid-poor particles will be formed in which the membrane protein cannot be reconstituted with high stability.[4,11,15] On the other hand, if the lipid to MSP ratio is too high, larger particles in the form of small vesicles will be formed. Besides an optimal membrane protein to MSP to lipid ratio, the size of the nanodisc can be of importance in case conformational changes of the membrane protein are required for functionality, and the right choice of lipid needs to be made if specific lipids are essential.

In this chapter, we describe the optimization of the reconstitution of the ECF NiaX transporter for niacin from *L. lactis* and of ECF FolT2 from *L. delbrueckii*. The biotin transporter BioMNY from *Rhodobacter capsulatus*, belonging to the group I ECF transporters, has been reconstituted in nanodiscs previously,[16] but this is the first report on the reconstitution of members from the group II ECF transporters in nanodiscs. Since S-components need to be exchanged during the transport cycle in case of the group II ECF transporters, our transporters might need more space within the nanodiscs to enable transport. The nanodisc formation is analyzed by size-exclusion chromatography and SDS-PAGE analysis, and the protein activity is checked using the ATPase activity assay described in Chapter 5.[17] The research started off with ECF NiaX, but since a higher protein yield could be obtained for ECF FolT2, the focus was switched to this transporter.

Results

Reconstitution of ECF NiaX in nanodiscs.

For the reconstitution of purified ECF NiaX from *L. lactis*, we started off with the membrane scaffold protein MSP1D1, which should yield nanodiscs with a diameter of about 97 Å.[11] The diameter of the transmembrane part of ECF FolT2 transporter from *L. delbrueckii* is roughly 50 to 60 Å over the longest axis.[17] Taking into account that conformational changes of the S-component and EcfT within the membrane might be required upon substrate translocation, nanodiscs with this diameter should be suitable to accommodate functional ECF NiaX.

For the lipid composition of the nanodiscs, two available ratios of synthetic lipids 1,2-dioleoyl-sn-glycero-3-phosphatidylcholine (DOPE) : 1,2-dioleoyl-sn-glycero-3-phosphatidylethanolamine (DOPC) : 1,2-dioleoyl-sn-glycero-3-phosphatidylglycerol (DOPG) of 60:20:20 and 50:12:38 have been used. With the first lipid composition, an optimal ECF NiaX:MSP1D1:lipid ratio of 1:5:500 was found. The size-exclusion chromatography (SEC) profile of the nanodiscs from this ratio shows two main peaks of nanodiscs with slightly different sizes (retention volumes of 10.2 mL and 11.4 mL, respectively, see the two arrows in Figure 2A, blue curve), accompanied by a peak at the void volume of the column (retention volume of 8.5 mL) and a shoulder (retention volume of 13 mL). According to SDS-PAGE analysis of the SEC fractions (Figure 2C), both peaks contain nanodiscs with the ECF NiaX transporter, although the band of NiaX in the second peak (retention volume of 11.4 mL) seems to be a bit less intense compared to the first peak. This can imply that the second main peak also contains nanodiscs with not complete ECF NiaX complexes. A previous study on the reconstitution of the ABC transporter OpuA in nanodiscs with the same membrane scaffold protein has shown that the SEC fractions at the void volume contain non-symmetric, donut-shaped structures with a diameter of about 20 nm.[18] These particles are most probably formed by the excess of lipids, which will form some kind of vesicles with the proteins that are not included in nanodiscs. The shoulder has about the same retention volume as the empty nanodiscs formed from the ECF NiaX:MSP1D1:lipid ratio of 0:5:500 (Figure 2B, blue curve) and will probably contain empty nanodiscs without ECF NiaX.

In case of lowering the amount of lipids to a ratio of 1:5:400 (Figure 2A, black curve, which has shifted compared to the blue curve due to technical problems), the second main peak (retention volume of 12 mL) with the nanodiscs of smaller size becomes a bit more abundant, while the opposite is true for the 1:5:600 ratio (Figure 2A, red curve). This shift in size is also seen in the SEC profile of the corresponding empty nanodiscs (indicated by the arrows in Figure 2B), suggesting the partition of a higher number of lipids in the nanodiscs when starting off with a higher fraction of lipids.

When changing to the lipid composition DOPE:DOPC:DOPG of 50:12:38 and the ECF NiaX:MSP1D1:lipid ratio to 1:10:1000, the peak at the void volume increased enormously (indicated by the arrow in Figure 2D, black curve,). Compared to 1:5:500 ratio, the peak of the empty nanodiscs (retention volume of 13 to 14 mL) increased too with respect to the peak with ECF NiaX nanodiscs (retention volume of 10.5 to 12 mL), indicating that the amount of MSPs and lipids is way too high in the 1:10:1000 ratio and results in the formation of other lipid-rich particles. Under the same conditions, the ATPase inactive mutant ECF NiaX EcfA E166Q EcfA' E'170Q has been reconstituted in nanodiscs. Also for this reconstitution, as well as in the preparation of empty nanodiscs

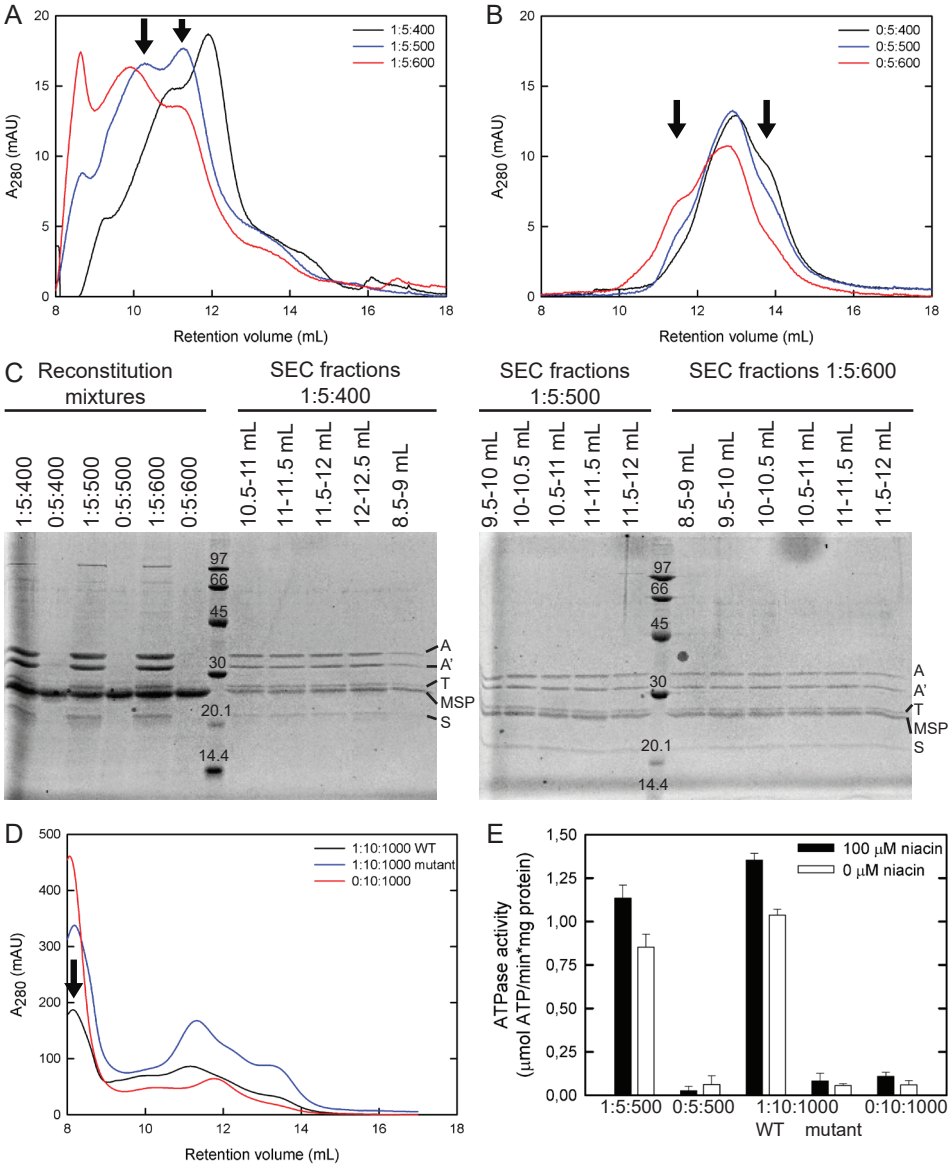

Figure 2: Reconstitution of ECF NiaX into nanodiscs. A) Size-exclusion chromatography (SEC) profile of the purification of the ECF NiaX nanodiscs from the reconstitution mixtures of ECF NiaX:MSP1D1:lipid of 1:5:400 (black), 1:5:500 (blue) and 1:5:600 (red). B) Same as in panel A for the empty nanodiscs from the reconstitution mixtures of ECF NiaX:MSP1D1:lipid of 0:5:400 (black), 0:5:500 (blue) and 0:5:600 (red). C) SDS-PAGE gels of the reconstitution mixtures and fractions from the SEC purification of the nanodiscs. The MSP1D1 and the EcfA, EcfA', EcfT and NiaX subunits of ECF NiaX are indicated by MSP, A, A', T and S, respectively. D) SEC profiles of the purification of nanodiscs with wild type ECF NiaX (black), the ECF NiaX EcfA E166Q EcfA' E170Q mutant (blue) and the empty nanodiscs (red), formed from reconstitution mixtures of ECF NiaX(wild type or mutant):MSP1D1:lipid of 1:10:1000 or 0:10:1000. E) ATPase activity of the nanodiscs from different reconstitution mixtures, measured in the presence (black bars) and in the absence (white bars) of 100 μM niacin. For the 1:10:1000 ECF NiaX:MSP1D1:lipid ratio, WT and

mutant indicate the activity of wild type ECF NiaX and the ECF NiaX EcfA E166Q EcfA' E'170Q mutant. The error bars represent the standard deviation from three measurements. The arrows in panels A, B and D indicate peaks to which is referred in the text.

from the 0:10:1000 ratio, the formation of other lipid-rich particles was observed (Figure 2D, blue and red curves).

ATPase activity of ECF NiaX reconstituted in nanodiscs.

ECF NiaX reconstituted in nanodiscs formed under the 1:5:500 reconstitution ratio, showed ATPase activity in the coupled-enzyme ATPase activity assay both in the absence and in the presence of 100 μM of its substrate niacin, with the activity being lowered by 25 % in the absence of niacin (Figure 2E). Although the preparation of nanodiscs under the 1:10:1000 ratio was not optimal, the ATPase activity of ECF NiaX in nanodiscs from this ratio was comparable with the one of the 1:5:500 ratio, and the same decrease in the absence of niacin was observed. This indicated that the ATPase activity of ECF NiaX is not dependent on one of the two lipid composition that we tested. When reconstituting the ATPase inactive mutant ECF NiaX EcfA E166Q EcfA' E170Q under the same conditions (lipid composition DOPE:DOPC:DOPG of 50:12:38 and the ECF NiaX:MSP1D1:lipid ratio to 1:10:1000), the activity was lowered to background values measured in the presence of empty nanodiscs, confirming that this mutant is not able to hydrolyze ATP.

Reconstitution of ECF FolT2 in nanodiscs.

For the reconstitution of ECF FolT2 from *L. delbrueckii* in nanodiscs, initially the same ECF FolT2:MSP1D1:lipid ratio of 1:5:500 as for ECF NiaX was used, with synthetic lipid composition DOPE:DOPC:DOPG of 60:20:20. This resulted in low ATPase activity (0.1 μmol ATP hydrolyzed per minute per mg of ECF FolT2) and no clear bands of the ECF FolT2 subunits were seen on the SDS-PAGE gel when analyzing the SEC fractions. Taking into account that the S-component needs to topple over and also might need to dissociate from the ECF module during the transport cycle, we switched to the larger membrane scaffold protein MSP2N2. This MSP would form nanodiscs with a diameter of 170 Å, in which the diameter of the lipid bilayer would be 145 Å.[13] Since these nanodiscs would need to contain more lipids, we tried different ECF FolT2:MSP2N2:lipid ratios (Table 1). For the ratios of 1:5:1800, 1:5:2000 and 1:5:2200, the SEC profiles showed a big peak at the void volume of the column (Figure 3A), while the SEC fractions with retention volumes of 9-10 mL and 11-11.5 mL (indicated by arrows in Figure 3A) showed to contain the MSP2N2, EcfA, EcfA', EcfT and FolT2 proteins in a ratio of about 2:1:1:1:1 (Figure 3B), implying one ECF FolT2 transporter incorporated per nanodisc surrounded by two MSP2N2 proteins.

In order to get rid of the big peak at the void volume, the number of lipids was lowered. At the same time, the lipid composition was changed to *E. coli* lipids:egg PC of 3:1, since this lipid composition was successfully used in the reconstitution of ECF FolT2 in proteoliposomes (see Chapter 5).[17] Analysis of the nanodisc formation from reconstitution mixtures with ECF FolT2:MSP2N2:lipid ratios of 1:4:750, 1:4:1000, 1:4:1250 and 1:4:1500 showed differences in abundance of the two peaks with retention volumes between 9 and 12 mL (indicated by the arrows in Figure 3C). For the 1:4:750

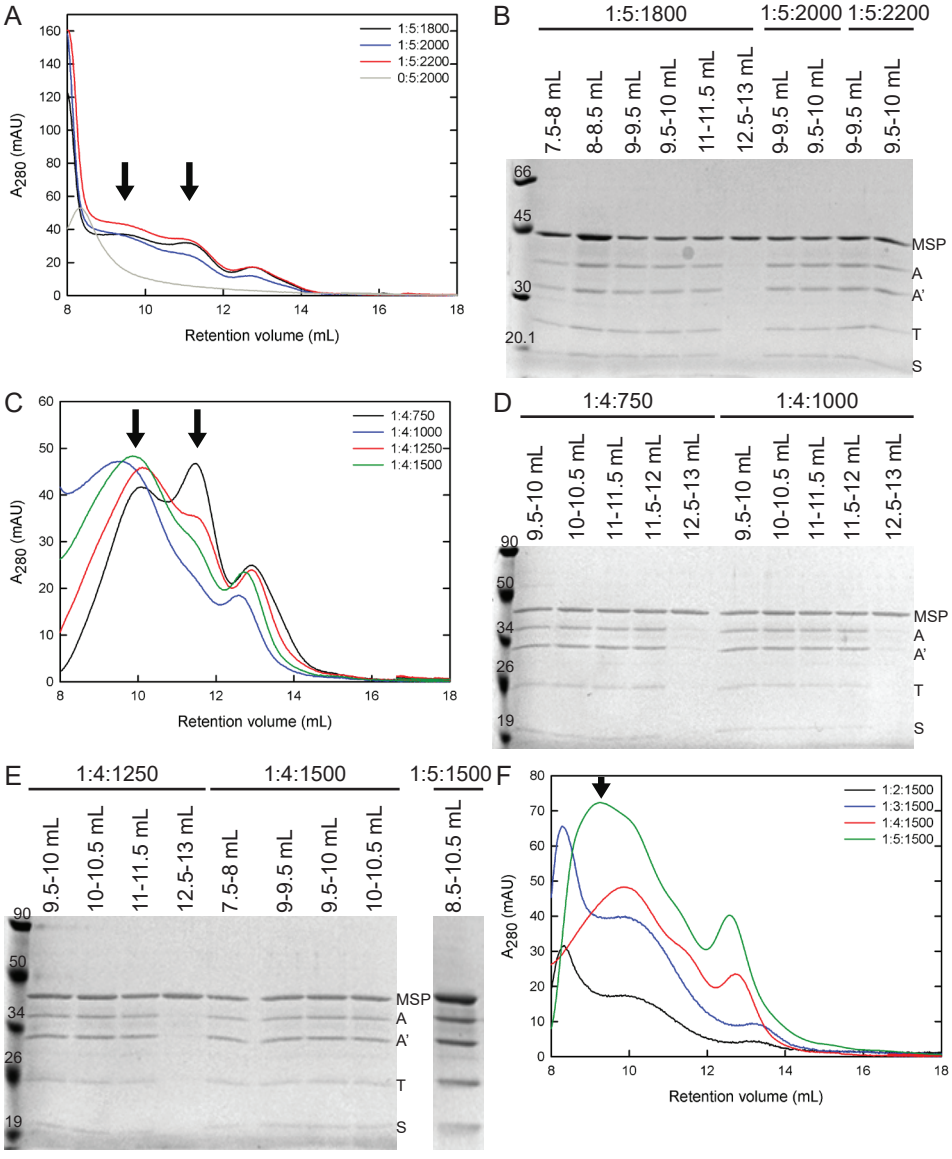

Figure 3: Reconstitution of ECF FolT2 in nanodiscs. A) SEC profile of the purification of the ECF FolT2 nanodiscs and empty nanodiscs from the reconstitution mixtures of ECF FolT2:MSP2N2:lipid of 1:5:1800 (black), 1:5:2000 (blue), 1:5:2200 (red) and 0:5:2000 (gray). B) SDS-PAGE gel of fractions from the SEC purifications of nanodiscs from panel A. C) Same as in panel A for the reconstitution mixtures of ECF FolT2:MSP2N2:lipid of 1:4:750 (black), 1:4:1000 (blue), 1:4:1250 (red) and 1:4:1500 (green). D-E) SDS-PAGE gel of fractions from the SEC purifications of nanodiscs from panel C and from the SEC purification of the ECF FolT2:MSP2N2:lipid ratio of 1:5:1500 in Panel F. F) Same as in panel A for the reconstitution mixtures of ECF FolT2:MSP2N2:lipid of 1:2:1500 (black), 1:3:1500 (blue), 1:4:1500 (red) and 1:5:1500 (green). The arrows in panels A, C and F indicate peaks to which is referred in the text.

Table 1: Different protein:MSP:lipid mixtures tested for the reconstitution of ECF FolT2 in nanodiscs.

Membrane scaffold protein	Lipid composition	ECF FolT2:MSP:lipid ratio
MSP1D1	DOPE:DOPC:DOPG of 60:20:20	1:5:1500
MSP2N2	DOPE:DOPC:DOPG of 60:20:20	1:5:1800 1:5:2000 1:5:2200
MSP2N2	*E. coli*:egg PC of 3:1	1:3:1500 1:2:1500 1:4:750 1:4:1000 1:4:1250 1:4:1500 1:5:1500

ratio with the lowest amount of lipids, the later peak is more abundant, while higher amounts of lipids in the other ratios cause higher abundance of the first peak, which would contain bigger nanodiscs. Analysis of the SEC fractions on gel showed poorer staining of EcfT and FolT2 compared to EcfA and EcfA' (Figure 3D and 3E), but this phenomena has been seen more often and has to do with the fact that these membrane protein stain less well compared to the soluble nucleotide binding domains. However, the bands of EcfT and FolT2 from the 1:4:1500 ratio fractions seem to be a bit more pronounced, and therefore optimization was continued from this protein to lipid ratio by changing the number of MSP2N2 proteins in the reconstitution ratio.

When lowering the number of MSP2N2 proteins to ratios of 1:3:1500 and 1:2:1500, the peak at the void volume appears again and the peak with nanodiscs between 9 and 11.5 mL decreases, implying a lower amount of stable nanodiscs being formed (Figure 3F, black and blue curve). Analysis of the SEC fractions from these 1:3:1500 and 1:2:1500 ratios by SDS-PAGE gel did not show clear bands for the ECF FolT2 subunits, and no band for the MSP2N2 protein at all, which raises the question if nanodiscs were formed at all. The SEC profile of nanodiscs from the ECF FolT2:MSP2N2:lipid ratio of 1:5:1500 is similar to the one from the 1:4:1500 ratio, with a new peak at a retention volume of about 9.5 mL appearing (indicated by the arrow in Figure 3F, green curve). The ratio of MSP2N2, EcfA, EcfA', EcfT and FolT2 on SDS-PAGE is roughly 2:1:1:1:1, only the staining of FolT2 is not as pronounced as for the other three (Figure 3E). Considering the height peak of ECF FolT2 nanodiscs with an expected MSP:protein ratio of 2:1 as shown by SDS-PAGE, as well as the absence of a peak at the void volume, the 1:5:1500 reconstitution ratio was chosen to be the most optimal one.

ATPase activity of ECF FolT2 reconstituted in nanodiscs.

Taking the main fraction of the peaks with ECF FolT2 nanodiscs from all different reconstitution ratios, the ATPase activity was measured in the presence and in the absence of 100 μM of folate (Figure 4A). After the 1:3:1500 ratio, the nanodiscs from the 1:5:1500 and 1:4:1500 ratio show the highest activity. For the 1:3:1500 and 1:2:1500 ratio, the activity in the absence of folate is 52 % and 61 % higher than in the presence of

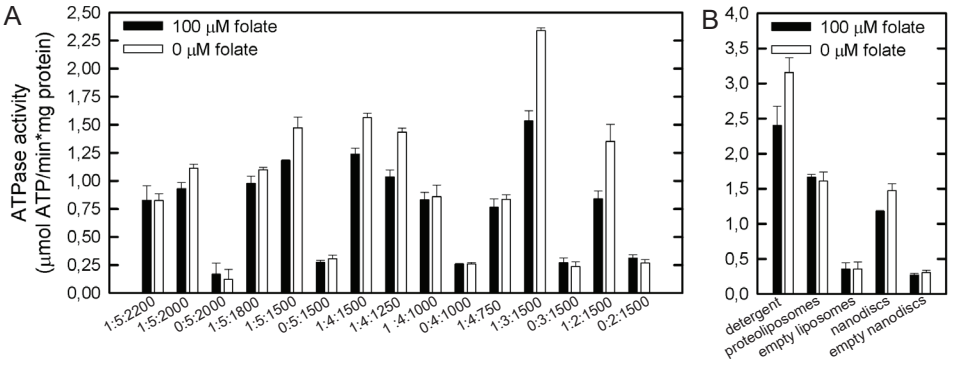

Figure 4: ATPase activity of ECF FolT2. A) ATPase activity of ECF FolT2 reconstituted in nanodiscs from different reconstitution mixtures, measured in the presence (black bars) and in the absence (white bars) of 100 µM of folate. Empty nanodiscs of five different ratios were taken along as well. The error bars represent the standard deviation from three measurements. B) ATPase activity assay of ECF FolT2 in detergent solution and reconstituted in proteoliposomes or nanodiscs, measured in the presence (black bars) and in the absence (white bars) of 100 µM of folate. The activity measured in the presence of empty liposomes and empty nanodiscs was taken along as well. The error bars represent the standard deviation from three measurements.

folate, while this difference is only 25 % and 26 % for the ratios 1:5:1500 and 1:4:1500, respectively. A similar difference of 31 % is seen in the ATPase activity of ECF FolT2 in detergent solution, while the ATPase activity of ECF FolT2 in proteoliposomes is similar in the presence and in the absence of folate (Figure 4B). In case of empty nanodiscs from different ratios and empty liposomes, the background ATPase levels are similar.

Discussion and conclusion

Although ECF NiaX from *L. lactis* and ECF FolT2 from *L. delbrueckii* both belong to the group II transporters for which the S-component is predicted to dissociate from the ECF module during the transport cycle, different MSPs needed to be used to get the transporters reconstituted in a functional way. For ECF NiaX, the smaller MSP1D1, which forms nanodiscs with a diameter of 95 Å, was used. However, ECF FolT2 turned out to be inactive when the same MSP1D1 and protein to MSP to lipid ratio was used as for ECF NiaX, implying that there is no "one size fits all" solution when reconstitution membrane proteins in nanodiscs, even not when working with similar proteins. This raised the question why ECF NiaX was satisfied with MSP1D1, while ECF FolT2 needed the larger MSP2N2.

When superimposing the crystal structure of folate-bound FolT1 from *L. delbrueckii* (PBD ID 5D0Y) with the structures of thiamine-bound ThiT (PDB ID 3RLB) and biotin-bound BioY from *L. lactis* (PDB ID 4DVE),[17,19,20] the dimensions were identical. This suggests that NiaX and FolT2 would not differ structurally that much from each other either. No crystal structure of a whole ECF transporter from *L. lactis* is available, so it is unknown if EcfT from *L. lactis* is structurally different from the one from *L. delbrueckii*. If it has a more compact structure compared to EcfT from *L. delbrueckii*, it is possible that the smaller nanodisc provides just enough space for the

conformational changes that need to occur to accommodate transport, while the same nanodisc is too small for the transporter from *L. delbrueckii*.

On the other hand, an explanation with regard to the biochemical properties of NiaX might be more plausible. Competition studies performed with NiaX and ThiT from *L. lactis* competing for interaction with the same ECF module for substrate transport, have shown that NiaX competes more efficiently for the ECF module than ThiT.[21] It is possible that NiaX has higher affinity for the ECF module in order to make niacin transport more efficient, because the uptake of niacin is preferred over the uptake of other substrates. In the absence of another S-component within the nanodisc, NiaX therefore does not dissociate from the ECF module. In case of FolT2, the affinity can be lower in comparison to the one for NiaX, with the consequence that FolT2 does dissociate during the transport cycle and therefore, ECF FolT2 requires more space within the nanodisc to complete the transport cycle.

When determining the ATPase activity of both transporters in the optimized nanodiscs, a drop in the ATPase activity of about 25 % was seen for ECF NiaX in the absence of its substrate niacin, while the ATPase activity was increased by about 25 % for ECF FolT2 in the absence of its substrate folate. This implies that there is no clear substrate dependence on the ATPase activity among these ECF transporters. When looking at the ATPase activity of ECF FolT2 in detergent solubilized state, the activity in the absence of folate is 31 % higher compared to the activity in the presence of folate, and in the non-optimized ECF FolT2 nanodiscs from the protein to MSP to lipid ratios of 1:2:1500 and 1:3:1500, the activity in the absence of folate is even 52 % and 61 % higher than in the presence of folate. However, when ECF FolT2 was reconstituted in proteoliposomes, the activity was similar regardless of the presence of folate. In the detergent solubilized state, the detergent micelle does not provide the same stability and properties as a lipid bilayer would provide, and maybe the nanodiscs in this optimized state do not provide the same properties as a lipid bilayer in a proteoliposome or in a cell in order for the substrates to have no influence on the ATPase activity at all.

Besides the different effects of niacin and folate, the ATPase activities measured were four orders of magnitude higher compared to the transport activities previously measured for ECF NiaX and ECF FolT2 (Chapter 5) when reconstituted in proteoliposomes.[17,22] High futile ATPase activity has been observed for the biotin transporter BioMNY from *Rhodobacter capsulatus* as well, which belongs to the group I ECF transporters.[16] As mentioned in Chapter 5 already, the high turnover of ATP by the ECF module might be accepted to make sure that the ECF module is in the right conformation to interact with a substrate-bound S-component as soon as it has captured its substrate, thereby making substrate transport efficient and giving the cell the ability to scavenge as much of the scarcely available nutrients as needed. However, it is still unknown if these high levels of futile ATP hydrolysis occur *in vivo* too.

To conclude, the research in this chapter has shown how to optimize the reconstitution of ECF transporters in nanodiscs while maintaining their activity, resulting a new model membrane system to study the ATPase activity of ECF transporters.

Experimental section

Expression and purification of ECF NiaX complexes.

ECF NiaX and the ECF NiaX EcfA E166Q EcfA' E170Q mutant have been cloned in the p2BAD vector previously and the vectors were transformed to *E. coli* MC1061 cells.[22,23] Cultivation was performed aerobically in 10 L of Yeast Trypton medium (8 g/L Bacto™ trypton, 5 g/L Bacto™ yeast extract, 2.5 g/L NaCl) supplemented with 100 µg/mL ampicillin in a 15 L fermenter at 37°C, 500 rpm, 30 % air. At OD_{600} of ~1.6, the temperature was lowered to 25°C and after allowing the cell culture to cool down for 20 minutes, expression was induced by addition of $1.5*10^{-3}$ % (v/v) of L-arabinose. One hour after induction, 0.2 % of glycerol was added to the cell culture. After 2.5-3 hours of expression, the cells were harvested by centrifugation (15 min, 7,446 x *g*, 4°C), washed and resuspended in buffer A (50 mM KPi, pH 7.5), and stored at -80°C after flash-freezing in liquid nitrogen. Before cell disruption, the cells were thawed and ~50 µg/mL of DNase, 1 mM of $MgCl_2$ and 1 mM of PMSF were added. The cells were lyzed by high-pressure disruption (Constant Cell Disruption System Ltd, UK, one passage at 25 kPsi, 5°C) and the cell debris was removed by low-speed centrifugation (30 min, 27,167 x *g*, 4°C). Membrane vesicles were pelleted by high-speed centrifugation (90 min, 185,677 x *g*, 4°C), and resuspended in buffer A to a total protein concentration of 15 mg/mL, as determined by Bradford Protein Assay (Bio-Rad). After aliquoting the membrane vesicles, they were flash-frozen in liquid nitrogen and stored at -80°C.

For the purification of the ECF NiaX proteins, membrane vesicles were thawed rapidly and solubilized in buffer C (50 mM KPi, pH 7.5, 300 mM NaCl, 10 % glycerol, 1 % (w/v) *n*-dodecyl-β-D-maltopyranoside (DDM, Anatrace)) for one hour at 4°C, while gently rocking. Unsolubilized material was removed by centrifugation (30 min, 285,775 x *g*, 4°C). The supernatant was incubated for one hour at 4°C under gently rocking with Talon resin (column volume of 1.1 mL), which had been equilibrated with buffer D (50 mM KPi, pH 7.5, 300 mM NaCl, 10 % glycerol, 10 mM imidazole, 0.05 % (w/v) DDM). Subsequently, the suspension was poured into a 10 mL disposable column (BioRad) and the flow through was collected. The column material was washed with 22 mL of buffer D. The ECF NiaX complexes were eluted in three fractions of 750 µL of buffer E (50 mM KPi, pH 7.5, 300 mM NaCl, 300 mM imidazole, 0.05 % (w/v) DDM). 1 mM of EDTA was added to the second elution fraction to remove co-eluted Ni^{2+} ions. Subsequently, the second elution fraction was purified by size-exclusion chromatography, using a Superdex 200 10/300 gel filtration column (GE Healthcare), equilibrated with buffer F (50 mM ammonium bicarbonate, pH 7.5, 150 mM NaCl, 0.05 % (w/v) DDM).

Expression, purification and reconstitution of ECF FolT2 complexes in proteoliposomes.

The expression, purification and reconstitution of the ECF FolT2 complexes in proteoliposomes has been performed as described in Chapter 5 using buffer G (50 mM KPi, pH 7.5, 150 mM NaCl, 0.05 % (w/v) DDM) for size-exclusion chromatography.[17]

Expression and purification of MSP1D1 and MSP2N2.

The pMSP1D1 and pMSP2N2 plasmids (Addgene plasmids 20061 and 26282, respectively) were purchased from Addgene and freshly transformed into Ca^{2+} competent cells of the *E. coli* BL21(DE3) strain before cultivation. For expression, the *E. coli* BL21(DE3) cells carrying the pMSP1D1 or pMSP2N2 plasmids were cultivated aerobically in 2 L of Terrific Broth medium (12 g/L Bacto™ trypton, 6 g/L Bacto™ yeast extract, 0.5 % glycerol) supplemented with 10 µg/mL of kanamycin, 17 mM KH_2PO_4 and 72 mM K_2HPO_4 in a 3 L fermenter (Applikon) at 37°C, 400-650 rpm, 50 % air.

Expression of MSP1D1 or MSP2N2 was induced at an OD_{600} of ~2 by addition of 1 mM of IPTG, and after three hours, the cells were harvested by centrifugation (15 min, 7,446 x *g*, 4°C). Subsequently, the cells were washed and resuspended in 200 mL of buffer H (50 mM KPi, pH 7.8) and stored at -80°C after flash-freezing in liquid nitrogen. Before cell disruption, 100 µg/mL of DNase and 1 mM of $MgSO_4$ were added to the thawed cells and after the cells were lysed by high-pressure disruption (Constant Cell Disruption System Ltd, UK, one passage at 25 kPsi, 5°C), 1 mM of PMSF and 1 % (v/v) of Triton X-100 (Sigma) was added. Cell debris was removed by low-speed centrifugation (30 min, 30,000 x *g*, 4°C) and 20 mM of imidazole was added to the supernatant.

For purification of MSP1D1 or MSP2N2, the supernatant was incubated for one hour at 4°C with Ni^{2+}-Sepharose column material (column volume = 7.5 mL for supernatant from 1 L of cell culture), which had been equilibrated with buffer H. The column material was then washed with 40 mL of each of the three following buffers: buffer I (40 mM Tris/HCl, pH 8.0, 0.3 M NaCl, 1 % (v/v) Triton X-100), buffer J (40 mM Tris/HCl, pH 8.0, 0.3 M NaCl, 50 mM Na-cholate, 20 mM imidazole) and buffer K (40 mM Tris/HCl, pH 8.0, 0.3 M NaCl, 50 mM imidazole). MSP1D1 or MSP2N2 was eluted in twelve elution fractions of 2 mL of buffer L (40 mM Tris/HCl, pH 8.0, 0.3 M NaCl, 500 mM imidazole), and the fractions that contained protein were combined and dialyzed overnight against 1 L of buffer M (20 mM Tris/HCl, pH 7.4, 0.1 M NaCl, 0.5 mM EDTA) to remove the imidazole. After filtering of the protein sample using a 0.22 µm syringe filter, it was diluted to a final protein concentration of 8 mg/mL and 0.01 % of NaN_3 was added. Subsequently, 500 µL aliquots of the purified protein were stored at -80°C.

Reconstitution into nanodiscs.

The reconstitution of the ECF transporters in phospholipid nanodiscs was performed as described previously with some modifications.[18] Briefly, liposomes with a synthetic lipid composition of DOPE:DOPC:DOPG of 50:12:38 were used for the reconstitution of the ECF NiaX complexes, while the liposomes with synthetic lipid composition of DOPE:DOPC:DOPG of 60:20:20 were used for both proteins, and liposomes with a lipid composition of *E. coli* polar lipid extract:egg PC of 3:1 were used only for the reconstitution of the ECF FolT2 complexes. The thawed liposomes were extruded through a 400 nm pore size polycarbonate filter (Avestin, eleven passages) and after addition of 1 % (w/v) of DDM, the mixture was vortexed until an optically clear solution was obtained. Purified ECF NiaX complexes, purified MSP1D1 and the destabilized liposomes were mixed in buffer N (50 mM KPi, pH 7.5, 12 mM DDM) to obtain different molar ratios as stated in the Results section, with the concentration of ECF NiaX varying from 1.4 µM to 4.3 µM and a concentration of 7.3 µM for the ATPase inactive ECF NiaX mutant (EcfA E166Q EcfA' E170Q). The purified ECF FolT2 complexes were mixed with purified MSP1D1 or MSP2N2 and the destabilized liposomes in buffer N to obtain the different molar ratios stated in the Results section with the concentration of ECF FolT2 varying from 1.4 µM to 5.0 µM. Subsequently, these reconstitution mixtures were incubated for 60 min at 4°C while gently rocking, after which 300 mg of Amberlite XAD-2 polymeric absorbent beads (Supelco, Sigma-Aldrich) were added. After incubation overnight at 4°C while gently rocking, the beads were removed by centrifugation (17,949 x *g*, 4°C) and the nanodiscs were purified from the supernatant by size-exclusion chromatography using a Superdex 200 10/300 gel filtration column (GE Healthcare), equilibrated with buffer O (50 mM KPi, pH 7.5, 150 mM NaCl). The fractions containing the nanodiscs were used directly or combined and

concentrated using a Vivaspin 500 concentrating device with a molecular weight cut-off of 100 kDa (Sartorius stedim) if no accurate protein concentration could be determined by Nanodrop. Subsequently, the nanodiscs were kept on ice until used, or frozen in liquid nitrogen and stored at -80°C.

ATPase activity assay.

The ATPase activity of the ECF transporters reconstituted in nanodiscs was measured by using a coupled enzyme assay described previously.[18] The assay was performed at 30°C in a 96-well plate, and the absorbance at 340 nm was measured by a Synergy MX-96 well plate reader (BioTek Instruments, Inc.). A standard experiment of 200 µL of reaction solution per well contained 50 mM KPi, pH 7.5, ~50 nM (1.2 µg) of ECF transporter, 4 mM of sodium phospho*enol*pyruvate, 0.3 mM of NADH and 3.5 µL of pyruvate kinase/lactic dehydrogenase enzyme mixture from rabbit muscle (Sigma-Aldrich) in 50 % glycerol. After incubation of the reaction solutions for 3 min at 30°C, 1 mM of MgATP, pH 7.5, was added to each of the reactions and the absorbance of NADH at 340 nm was followed for 7-10 min. The ATPase activity was expressed in µmol of ATP hydrolyzed/(min * mg of ECF transporter) and bar charts were prepared using SigmaPlot version 11 software.

References

1. Anatrace detergents. at <https://www.anatrace.com/Products/Detergents>
2. Sanders, C. R. & Landis, G. C. Reconstitution of Membrane Proteins into Lipid-Rich Bilayered Mixed Micelles for NMR Studied. *Biochemistry* **34,** 4030–4040 (1995).
3. Faham, S. & Bowie, J. U. Bicelle Crystallization : A New Method for Crystallizing Membrane Proteins Yields a Monomeric Bacteriorhodopsin Structure. *J. Mol. Biol.* **316,** 1–6 (2002).
4. Bayburt, T. H., Grinkova, Y. V. & Sligar, S. G. Self-Assembly of Discoidal Phospholipid Bilayer Nanoparticles with Membrane Scaffold Proteins. *Nano Lett.* **2,** 853–856 (2002).
5. Bayburt, T. H. & Sligar, S. G. Single-molecule height measurements on microsomal cytochrome P450 in nanometer-scale phospholipid bilayer disks. *Proc. Natl. Acad. Sci. U. S. A.* **99,** 6725–6730 (2002).
6. Knowles, T. J. *et al.* Membrane Proteins Solubilized Intact in Lipid Containing Nanoparticles Bounded by Styrene Maleic Acid Copolymer. **131,** 7484–7485 (2009).
7. Bayburt, T. H. & Sligar, S. G. Self-assembly of single integral membrane proteins into soluble nanoscale phospholipid bilayers. *Protein Sci.* **12,** 2476–2481 (2003).
8. Atkinson, D. & Small, D. M. Recombinant Lipoproteins: Implications for Structure and Assembly of Native Lipoproteins. *Annu. Rev. Biophys. Biophys. Chem.* **15,** 403–456 (1986).
9. Ohashi, R., Mu, H., Wang, X., Yao, Q. & Chen, C. Review Reverse cholesterol transport and cholesterol efflux in atherosclerosis. **98,** 845–856 (2005).
10. Boldog, T., Li, M. & Hazelbauer, G. L. Using Nanodiscs to create water-soluble transmembrane chemoreceptors inserted in lipid bilayers. *Methods Enzymol.* **423,** 317–35 (2007).
11. Denisov, I. G., Grinkova, Y. V, Lazarides, A. A. & Sligar, S. G. Directed self-assembly of monodisperse phospholipid bilayer Nanodiscs with controlled size. *J. Am. Chem. Soc.* **126,** 3477–87 (2004).

12. Ritchie, T. K. *et al. Chapter 11 - Reconstitution of membrane proteins in phospholipid bilayer nanodiscs. Methods in enzymology* **464,** (Elsevier Inc., 2009).

13. Grinkova, Y. V, Denisov, I. G. & Sligar, S. G. Engineering extended membrane scaffold proteins for self-assembly of soluble nanoscale lipid bilayers. *Protein Eng. Des. Sel.* **23,** 843–8 (2010).

14. Borch, J. & Hamann, T. The nanodisc: a novel tool for membrane protein studies. *Biol. Chem.* **390,** 805–14 (2009).

15. Bayburt, T. H. & Sligar, S. G. Membrane protein assembly into Nanodiscs. *FEBS Lett.* **584,** 1721–7 (2010).

16. Finkenwirth, F. *et al.* ATP-dependent Conformational Changes Trigger Substrate Capture and Release by an ECF-type Biotin Transporter. *J. Biol. Chem.* **290,** 16929–42 (2015).

17. Swier, L. J. Y. M., Guskov, A. & Slotboom, D. J. Structural insight in the toppling mechanism of an energy-coupling factor transporter. *Nat. Commun.* **7,** 11072 (2016).

18. Karasawa, A. *et al.* Physicochemical factors controlling the activity and energy coupling of an ionic strength-gated ATP-binding cassette (ABC) transporter. *J. Biol. Chem.* **288,** 29862–71 (2013).

19. Erkens, G. B. *et al.* The structural basis of modularity in ECF-type ABC transporters. *Nat. Struct. Mol. Biol.* **18,** 755–760 (2011).

20. Berntsson, R. P. *et al.* Structural divergence of paralogous S components from ECF-type ABC transporters. *Proc. Natl. Acad. Sci. U. S. A.* **109,** 13990–13995 (2012).

21. Majsnerowska, M., Beek, J., Stanek, W. K., Duurkens, R. H. & Slotboom, D. J. Competition between Different S-Components for the Shared Energy Coupling Factor Module in Energy Coupling Factor Transporters. *Biochemistry* **54,** 4763–4766 (2015).

22. Beek, ter, J., Duurkens, R. H., Erkens, G. B. & Slotboom, D. J. Quaternary structure and functional unit of energy coupling factor (ECF)-type transporters. *J. Biol. Chem.* **286,** 5471–5475 (2011).

23. Birkner, J. P., Poolman, B. & Koçer, A. Hydrophobic gating of mechanosensitive channel of large conductance evidenced by single-subunit resolution. *Proc. Natl. Acad. Sci. U. S. A.* **109,** 12944–12949 (2012).